SUPPORTING INFORMATION

Continuous Online Protein Quality Monitoring during Perfusion Culture Production Using an Integrated Micro/Nanofluidic System

Taehong Kwon[†,§,$], Sung Hee Ko[†,×,$], Jean-François P. Hamel[#,**], and Jongyoon Han[†,§,‡,ǁ,*]

[†]Research Laboratory of Electronics, Massachusetts Institute of Technology, MA 02142, USA

[§]Department of Electrical Engineering and Computer Science, Massachusetts Institute of Technology, MA 02142, USA

[#]Department of Chemical Engineering, Massachusetts Institute of Technology, MA 02142, USA

[‡]Department of Biological Engineering, Massachusetts Institute of Technology, MA 02142, USA

[ǁ]Critical Analytics for Manufacturing Personalized-Medicine (CAMP) IRG, Singapore-MIT Alliance for Research and Technology (SMART) Centre, Singapore

Corresponding Authors

*Email: jyhan@mit.edu

**Email: jhamel@mit.edu

Present Addresses

×Vaccine Research Center, National Institute of Allergy and Infectious Diseases, National Institute of Health, Bethesda, MD 20892, USA

$These authors contributed equally to this work.

Table of Contents

- Fabrication of the nanofluidic device
- Section 1. Nanofluidic online protein size monitoring system integrated with perfusion culture.
    - Figure S1. Perfusion culture of CHO cells using the microfluidic cell retention device.
    - Figure S2. High-concentration perfusion culture of CHO cells using the microfluidic cell retention device.
    - Method for perfusion culture using the microfluidic cell retention device
    - Figure S3. Online nanofluidic protein size monitoring system.
    - Figure S4. Continuous online buffer exchange and cell clarification.
    - Figure S5. Continuous online protein labeling, free dye removal, and protein denaturation.
    - Figure S6. Protein size monitoring by the nanofluidic filter array device.
- Section 2. Characterization of protein sizing in the nanofluidic device.
    - Figure S7. Offline separation of protein mixture in the nanofluidic device.
    - Table S1. Information about the proteins used for Figure S1.
    - Figure S8. Size analysis of standard IgG_1 by the microchip electrophoresis (Bioanalyzer 2100, Agilent).
- Section 3. Perfusion culture results.
    - Figure S9. Microfluidic cell retention performance and culture results during steady-state IgG_1 production.
    - Figure S10. Microfluidic cell retention performance and culture results during transient-state IgG_1 production.
- Section 4. Nanofluidic monitoring results.
    - Table S2. Summary of the monitoring results during perfusion culture.
- Section 5. Online sample preparation test, technology comparison, and monitoring delay
    - Figure S11. Test of online sample preparation in terms of proportion of each size group
    - Figure S12. Offline and online denaturation of standard IgG_1 and culture supernatant produced from the perfusion bioreactor
    - Table S3. Comparison with other technologies (mAb fragment and aggregation)
    - Table S4. Processing time delay of online sample preparation and possible solutions
- Section 6. Effect of electric field strength on separation performance of the nanofluidic device.
    - Figure S13. Offline separation of IgG_1 and protein mixture in the nanofluidic device at 100 V.
    - Separation performance of biomolecule mixtures is affected by electric field strength (voltage)

- Section 7. Figure data.
    - Table S5. Figure data for Figure 4 and 5.
- References

Fabrication of the nanofluidic device

The nanofluidic device (slanted nanofilter array) was fabricated through multiple standard MEMS fabrication methods. To make the nanofilter array on a silicon substrate, photolithography by a stepper with a 5X reduction (NSR2005i9, Nikon Precision Inc.) and dry etching by reactive ion etching (RIE) were used. The access holes to load samples and apply electric field were made by wet etching using potassium hydroxide (KOH). A thermal oxide layer (SiO_2) was grown on the silicon substrate for electrical insulation between the silicon substrate and buffer solution. Fusion bonding method was used to bond the silicon and glass (Pyrex) substrates to prevent nanochannel collapse because the aspect ratio of width and depth in the nanochannel was small. As a final step, the bonded substrates were cut by die saw machine.

Section 1. Nanofluidic online protein size monitoring system integrated with perfusion culture.

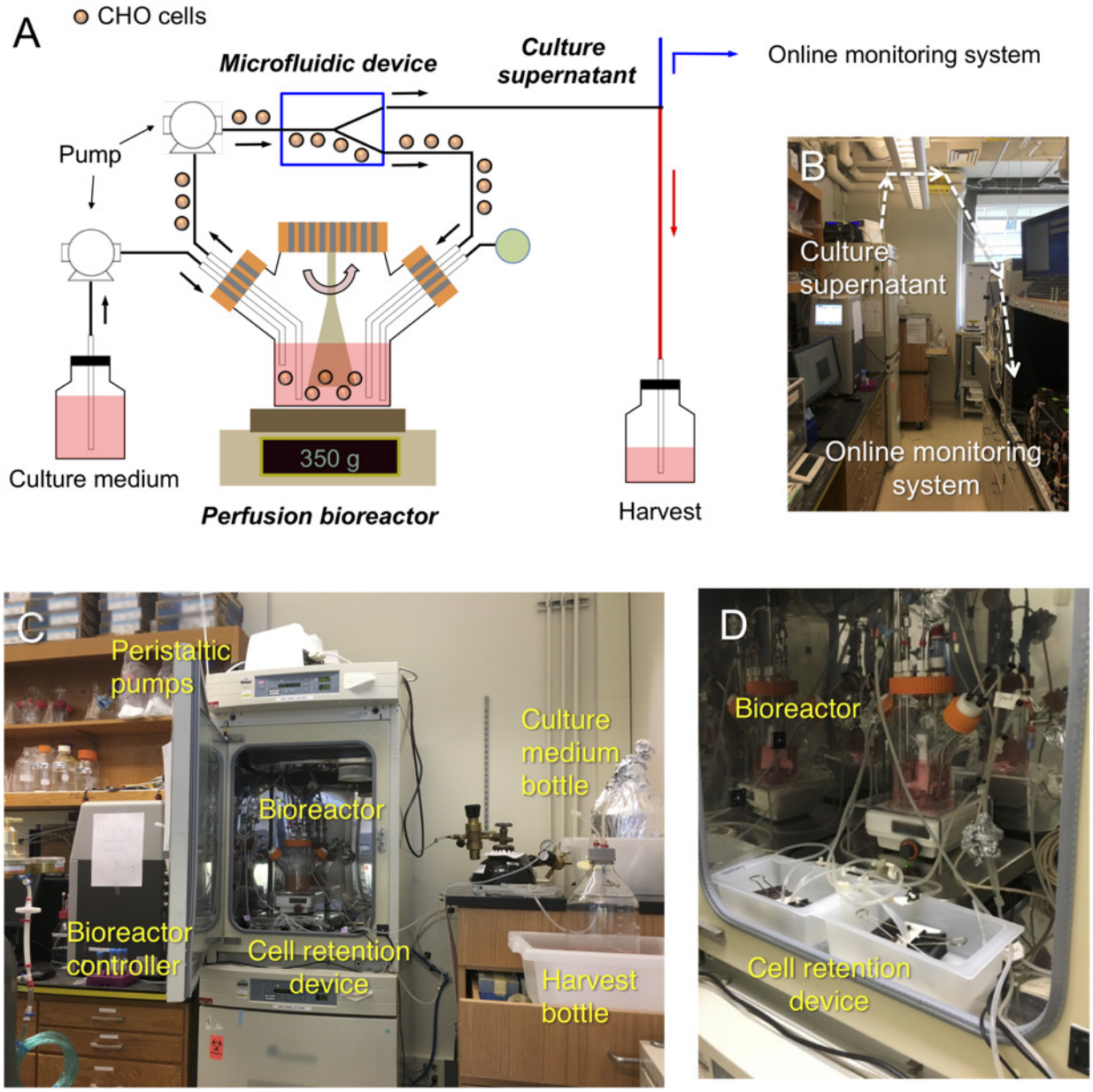

Figure S1. Perfusion culture of CHO cells using the microfluidic cell retention device. (**A**) System schematic for perfusion culture. (**B**) Continuous culture supernatant flow from the perfusion bioreactor to the online monitoring system. (**C**) The picture of actual perfusion culture system. (**D**) The bioreactor and cell retention devices. One of the cell retention devices was used as a back-up device.

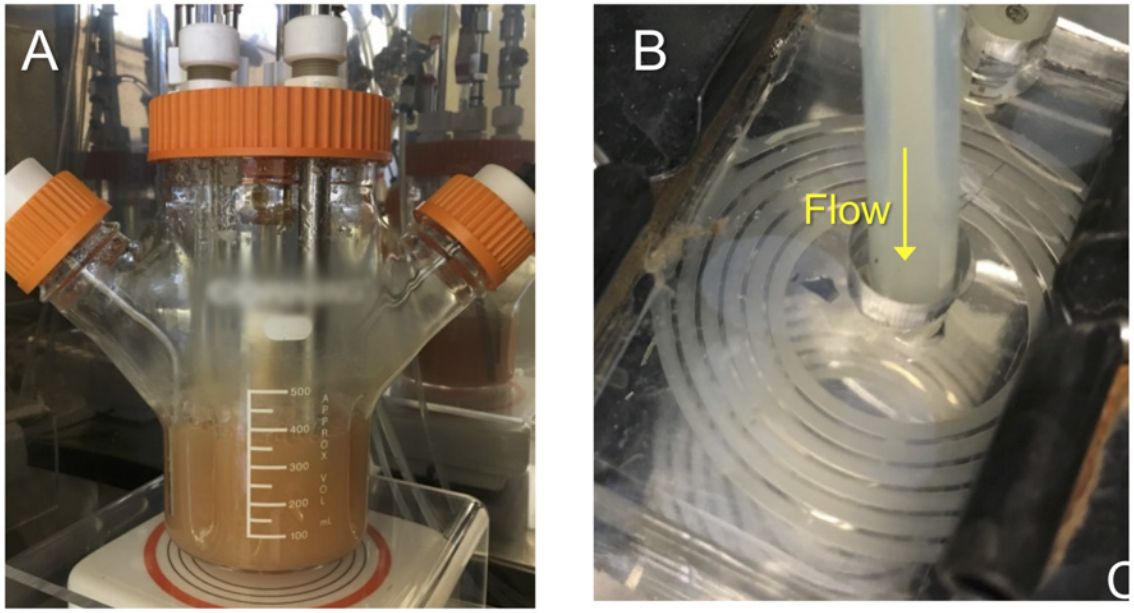

Figure S2. High-concentration perfusion culture of CHO cells using the microfluidic cell retention device. (**A**) High-cell-concentration (29×10^6 total cells/mL with 93% cell viability) perfusion bioreactor. (**B**) The spiral microfluidic cell retention device in operation.

Method for perfusion culture using the microfluidic cell retention device

CHO cells were grown in a customized spinner flask whose working volume was 350 mL. The pH (7.0) and dissolved oxygen (40%) of the bioreactor were automatically controlled by a commercial bioreactor controller (BIOSTAT® A PLUS, Sartorius Stedim North America Inc.). Sodium bicarbonate (7.5%) solution (S8761, MilliporeSigma) was used as a base solution. The detailed procedures for fabrication of the microfluidic cell retention and perfusion culture were described before.[1] Perfusion began on day 3 with a rate of 700 mL day^{-1} (two bioreactor volumes per day). Fresh cell culture medium (CD OptiCHO™, 12681011, Thermo Fisher Scientific) was continuously supplied into the bioreactor while cell culture supernatant containing monoclonal antibodies (IgG_1) and toxic metabolites were removed by the microfluidic cell retention device. The culture harvest removed from the bioreactor was collected in a harvest bottle, which was replaced daily. Most of the cells (>98.5%) were maintained in the bioreactor and reached high cell concentration (20–40 million cells mL^{-1}). They continuously produced monoclonal antibodies (IgG_1). Cell culture was sampled daily and, cell culture parameters, such as cell concentration, viability, live cell diameter, pH, glucose and lactate concentrations, and oxygen level, were measured by the automated cell culture analyzer (FLEX II, NovaBiomedical).

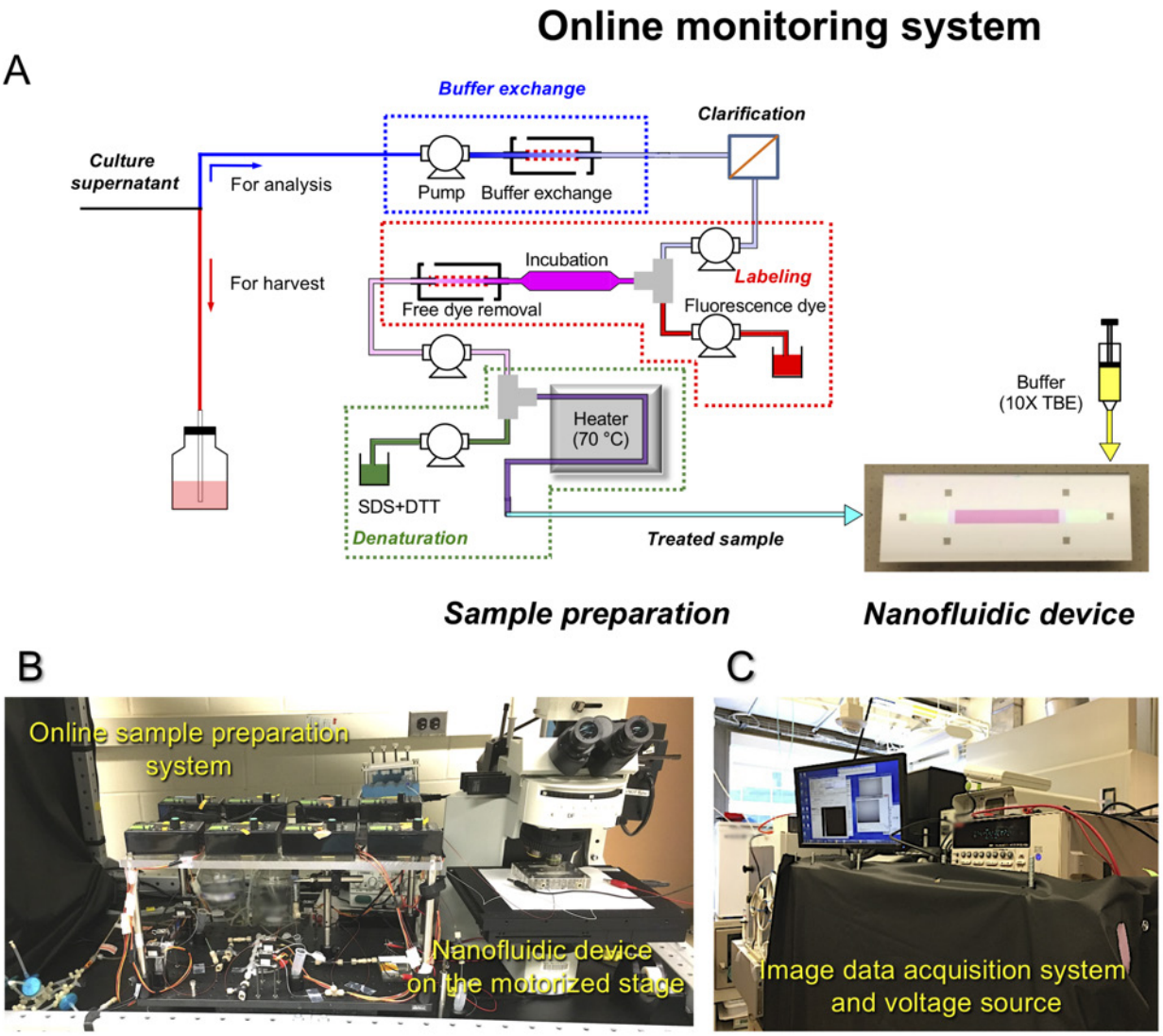

Figure S3. Online nanofluidic protein size monitoring system. (**A**) System schematic for online monitoring system. (**B**) Online sample preparation system and nanofluidic device on the motorized stage. The photo shows fluid handling parts (peristaltic pumps and capillary tubes), an upright microscope, and nanofluidic device in the dark room. The nanofluidic device in the device holder was placed on the motorized stage. (**C**) Image data acquisition system and voltage source on the dark room.

For detection of proteins in the supernatant in the nanofluidic device, proper sample treatment process depending on target is required. The online sample preparation consists of buffer-exchange, cell clarification, protein labeling, free (unbound) dye removal, and protein denaturation (**Figure 3B**; **Figure S3–S5**).

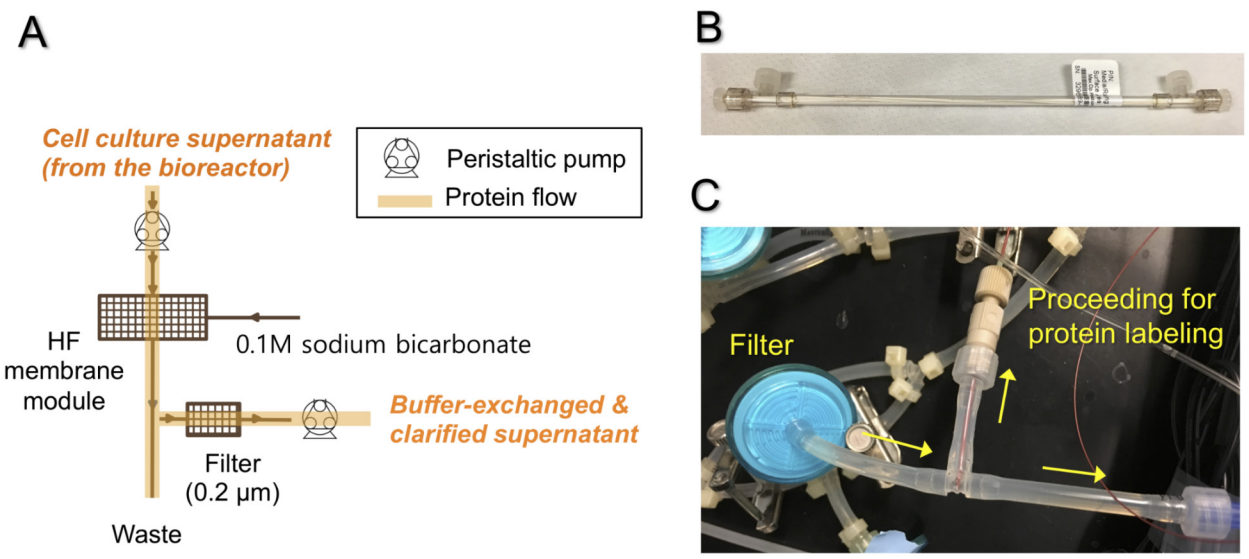

Figure S4. Continuous online buffer exchange and cell clarification. (**A**) System schematic for continuous online buffer exchange and cell clarification. (**B**) A sterile hollow fiber membrane module for buffer exchange. (**C**) Continuous cell clarification (removal of cells and cell debris) through a 0.2 μm filter. The buffer-exchanged and clarified supernatant proceeded to the protein labeling step (**Figure S5**).

For buffer-exchange (**Figure S4**), a sterile hollow fiber membrane module (C02-E003-05-S, Spectrum Laboratories) was used with 0.1M sodium bicarbonate (S66014-1kg, Sigma-Aldrich). Its molecular weight cut-off (MWCO) was 3 kDa, and the inner diameter of the fiber was 0.5 mm. The membrane was made of modified polyethersulfone (mPES), and its surface area was 20 cm^2.

Subsequently, cell clarification was performed to remove cells and cell debris from the buffer-exchanged solution (**Figure S4**). The CHO cells (10–20 μm) or cell debris (<10 μm) could easily clog the small-diameter (<1 mm) plastic capillary/silicone tubes and the entrance of the nanofluidic device, interfering with reliable monitoring. The micro peristaltic pump (RP-TX series, Takasago Fluidic Systems) drew the buffer-exchanged solution continuously through a syringe filter (4658, Pall Laboratory) with 0.2 μm pore size and 32 mm diameter. Due to high cell retention efficiency (>98% in terms of total number of cells) by the microfluidic cell retention during perfusion culture, one syringe filter was used for long-term (~1 week) operation without filter replacement.

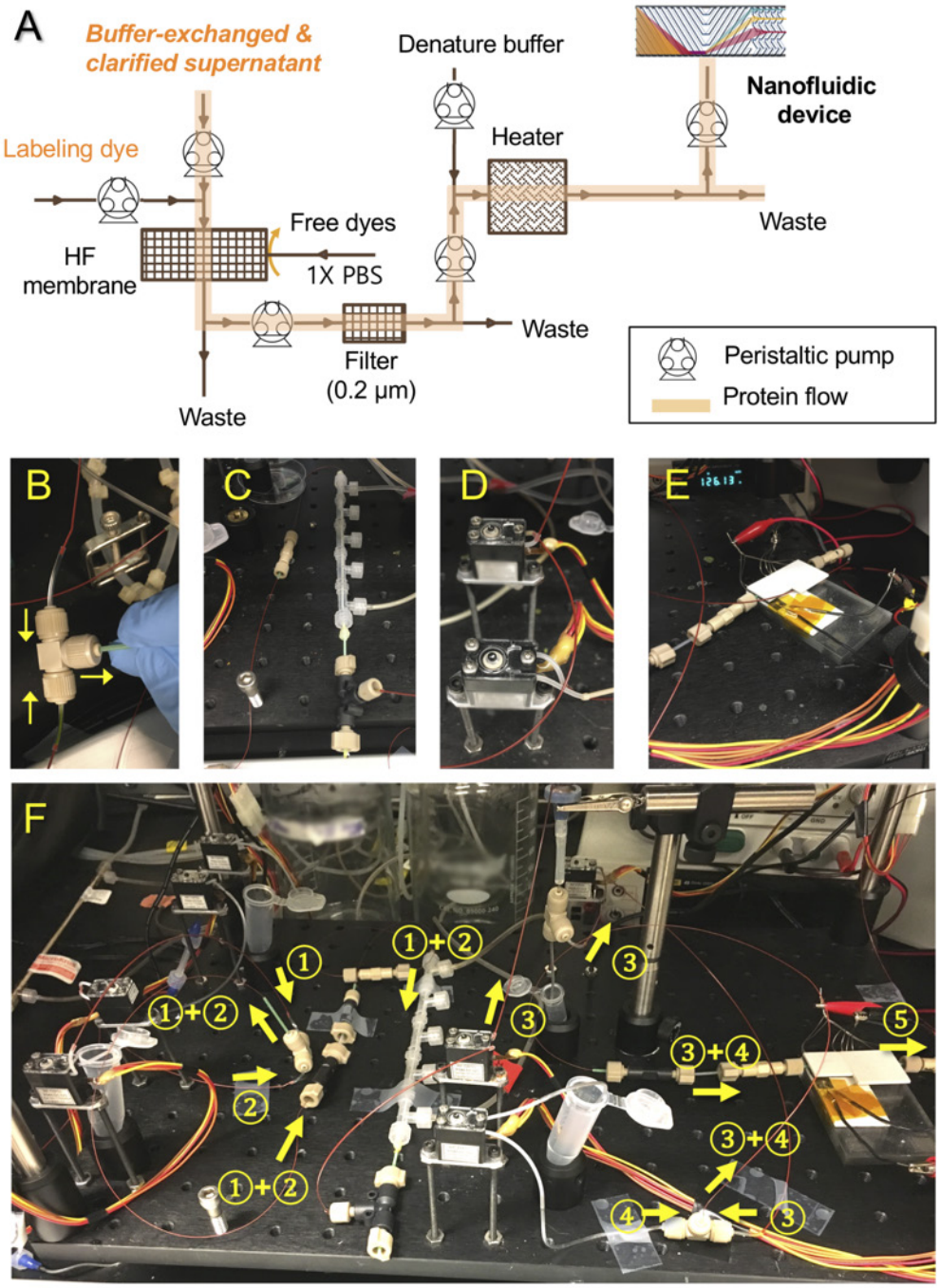

Figure S5. Continuous online protein labeling, free dye removal, and protein denaturation. (**A**) System schematic. (**B**) Buffer-exchanged and clarified protein solution was mixed with the protein labeling dye after the capillary junction. (**C**) Customized hollow fiber membrane module for free dye removal. (**D**) Micro peristaltic pumps used to deliver samples and reagents during online sample preparation. (**E**) A ceramic heater used to heat and denature proteins. (**F**) #1: Buffer-exchanged and clarified proteins, #2: Protein labeling fluorescence dye, #3: Labeled proteins after free dye removal, #4: Denaturing solution, #5: Denatured proteins prior to nanofluidic monitoring.

A customized hollow fiber membrane with reduced internal volume was used to remove free dyes from the protein-dye mixture (**Figure S5**). The hollow fiber from the module (C06-E005-05-N, Spectrum Labs) was cut off and inserted into Luer fittings (64-1579, 64-1578, Warner Instruments). Subsequently, a PEEK tubing (1571, IDEX Health & Science) was inserted into the hollow fiber. An adhesive was applied to the tubing and fiber to hold the tubing and prevent leakage during continuous online free dye removal. The complete free dye removal setup was placed at room temperature for more than 24 hours to ensure fully curing of the adhesive. Finally, the free dye removal setup was connected to the online protein labeling setup. 10X PBS with pH 7.2 (70013032, Thermo Fischer Scientific) was diluted with deionized water by 10-fold to prepare 1X PBS. This 1X PBS was continuously flowed into the free dye removal setup to remove free dyes from the protein-dye mixture.

For protein denaturation (**Figure S5**), the denaturation solution was prepared using 1M Dithiothreitol (D1532, Thermo Fisher Scientific), 10X Tris-borate-EDTA buffer reagent (T4415-1L, Millipore Sigma), and sodium dodecyl sulfate (L3771-100G, Millipore Sigma). The final concentrations of the dithiothreitol (DTT) and sodium dodecyl sulfate (SDS) in the denaturing buffer solution were 11mM and 0.11%. The ready-to-use denaturing buffer was prepared in a 5mL MacroTubes (470225-006, VWR) and mixed with the labeled and purified protein solution in the PEEK tubing (1571, IDEX Health & Science). Afterwards, the solution was heated up with a metal ceramic resistive heater (HT24S2, Thorlabs) to denature the proteins. The resistance of the heater was controlled by a DC power supply, and the temperature was monitored by a resistance temperature detector (TH100PT, Thorlabs). The final labeled, purified, and denatured protein solution was fed into the nanofluidic filter array device to monitor its size distribution.

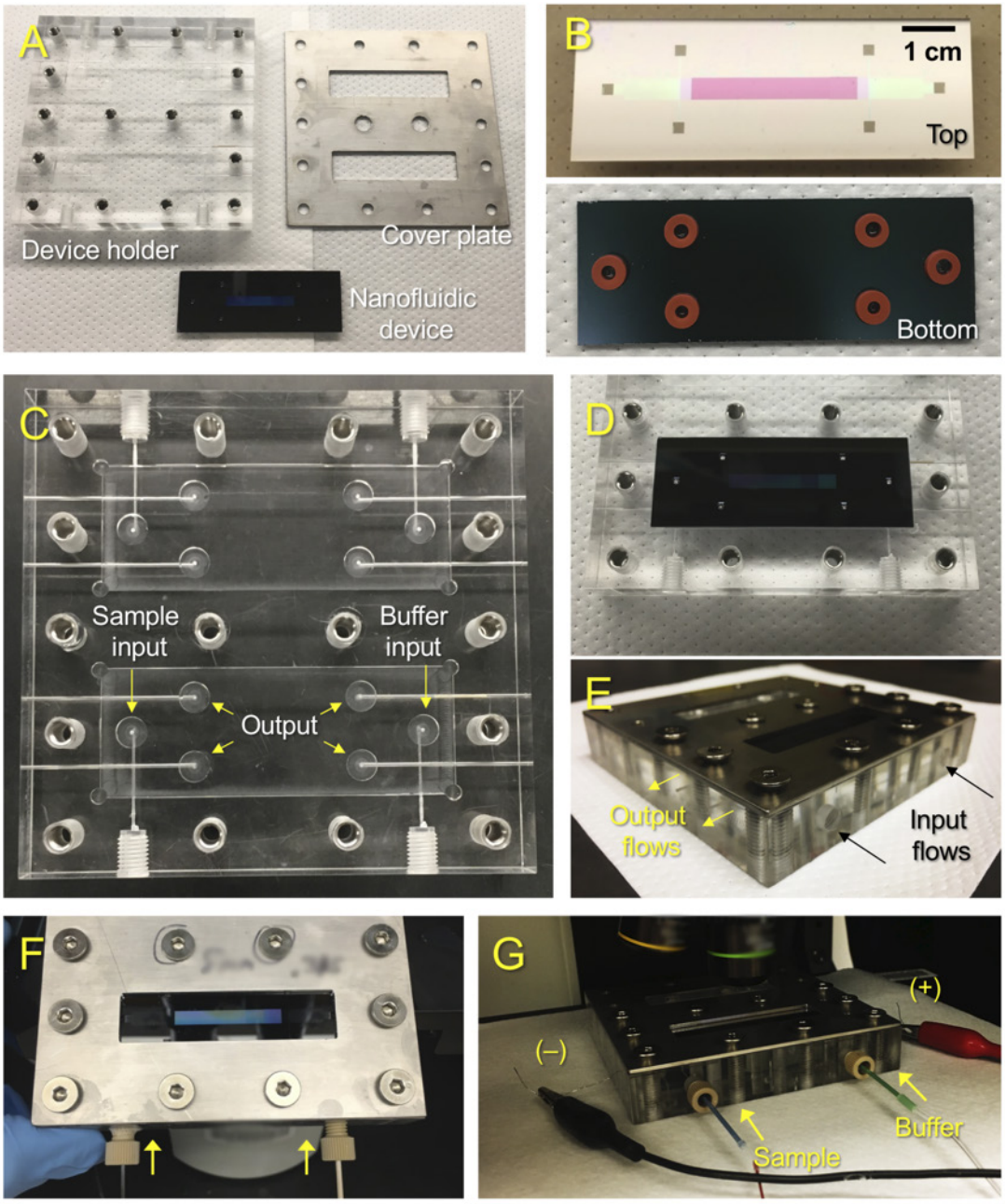

Figure S6. Protein size monitoring by the nanofluidic filter array device. (**A**) The nanofluidic device and its holder for fluid delivery and voltage application. (**B**) The top and bottom views of the nanofluidic device. O-rings were attached to the reservoirs of the device. (**C**) The magnified view of the device holder. It was designed such that multi-modal protein quality analysis (*e.g.*, simultaneous size and bioactivity analyses) could be possible. (**D**) The nanofluidic device placed on the holder. (**E**) The holder possesses holes on its sides for the delivery of the input and output flows. (**F**) The top view of the nanofluidic device in the holder. (**G**) The device and its holder placed on the motorized stage. The voltage is applied to the output reservoirs of the device.

The metal cover was placed on top of the holder, and the reservoirs of the device were connected to the holes of the holder without any leakage by inserting rubber O-rings between reservoirs of the device and holes of the holder. The holder possessed six open channels. Three of them on one side were designed to flow the input protein mixture (one input channel; two output channels) while the rest of them on the other side were designed to flow the input buffer solution (10X TBE; one input channel; two output channels).

The final labeled, purified, and denatured protein solution from the online sample preparation was continuously fed into the sample input side of the nanofluidic device by a peristaltic pump (RP-TX series, Takasago Fluidic Systems). The 10X TBE buffer solution was flowed into the buffer input side of the device by a syringe pump at 1 μL min^{-1}. PEEK tube adaptors were used to connect sample flows to the holder of the nanofluidic device. Platinum electrodes (711000, A-M SYSTEMS) were inserted into the output reservoirs, and an electric field was applied to the nanofluidic device.

Section 2. Characterization of protein sizing in the nanofluidic device.

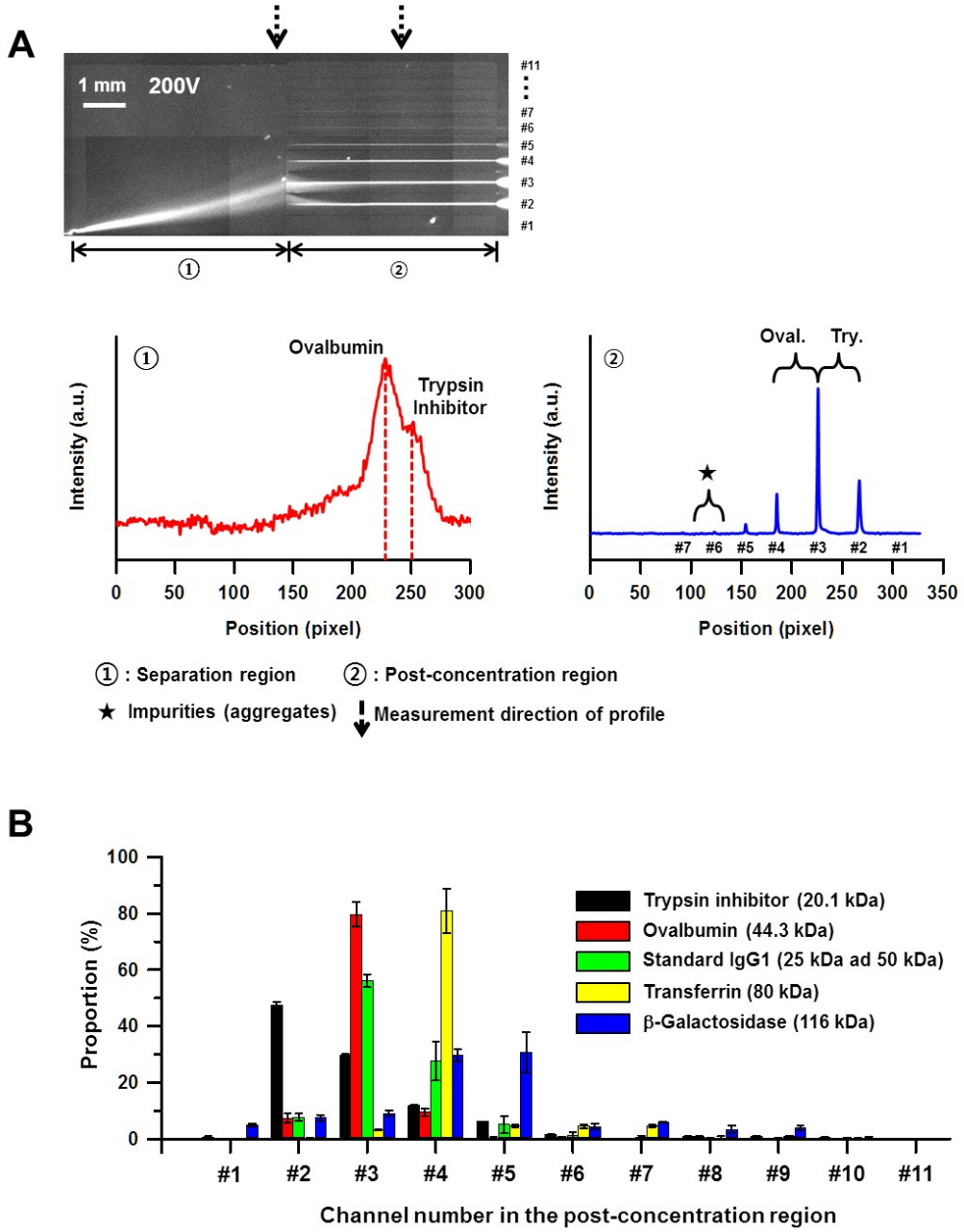

Figure S7. Offline separation of protein mixture in the nanofluidic device. (**A**) Separation of mixture of ovalbumin (44.3 kDa) and trypsin inhibitor (20.1 kDa) (500 μg mL^{-1}). The fluorescence image of proteins' behavior in the nanofluidic device and fluorescence signal profiles of separated proteins in the separation and post-concentration regions. 200 V was applied to the filter array. (**B**) Size distribution of various protein size markers and IgG_1 in the post-concentration channels. The **Table S1 (**see below**)** shows the detailed information about the proteins. 200 V was applied to the filter array. All the proteins were fluorescently labeled and denatured using SDS and DTT. Error bars, data range (n = 3).

The signal intensity of the certain protein size marker was dominant in the certain post-concentration channel. For example, the first and second highest peaks for the trypsin inhibitor (20.1 kDa) were in the post-concentration channels #2 and #3, respectively. The post-concentration channels #3 and #4 exhibited the first and second highest peaks, respectively, for both Ovalbumin (44.3 kDa) and standard IgG_1 (23.5 kDa of two light chains and 50 kDa of two heavy chains). Moreover, the post-concentration channels #4 and #5 contained most of the fluorescence signals coming from β-Galactosidase from E. coli (116 kDa).

Table S1. Information about the proteins used for Figure S1. The purity was measured with offline gel electrophoresis equipment (Bioanalyzer 2100, Agilent).

Protein	Molecular weight [kDa]	Vendor	Catalog number	Purity [%]
Trypsin inhibitor from Glycine max (soybean)	20.1	MilliporeSigma	T9767	83
Albumin from chicken egg white (Ovalbumin)	44.3	MilliporeSigma	A7642	96
IgG_1, Kappa from human myeloma plasma	23.5 (two light chains) and 50 (two heavy chains)	MilliporeSigma	I5154	94
Human transferrin	80	MilliporeSigma	T3309	87
β-Galactosidase from *Escherichia coli*	116.3 (one unit of the tetramer)	MilliporeSigma	G8511	79

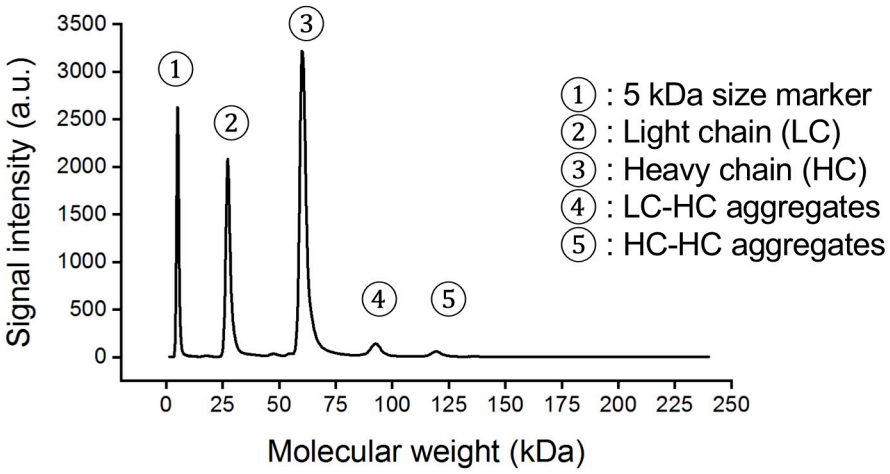

Figure S8. Size analysis of standard IgG_1 by the microchip electrophoresis (Bioanalyzer 2100, Agilent). Standard (purified) IgG_1 (I5154, MilliporeSigma) at 500 μg/mL was labeled and SDS-denatured under a reducing condition using dithiothreitol (DTT). The sample was prepared using the Agilent High Sensitivity Protein 250 Kit (5067-1575, Agilent). The sample contained light chain (LC) (②) and heavy chain (HC) (③). It also contained impurities (④: LC-HC aggregates, ⑤: HC-HC aggregates). ① represents a 5 kDa size marker which is contained in every sample. The proportion of IgG_1 (LC+HC) was 93.6 % ± 0.5 % (average ± s.d., n = 5) while that of impurities was 6.4 % ± 0.5 %.

Section 3. Perfusion culture results.

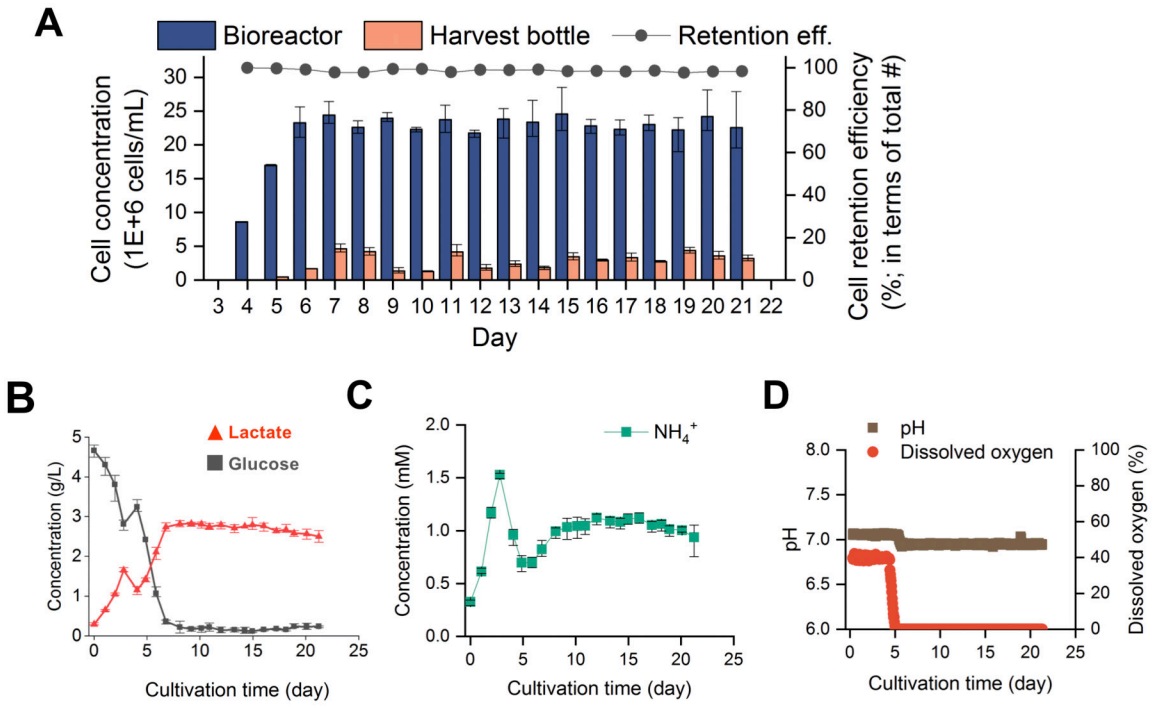

Figure S9. Microfluidic cell retention performance and culture results during steady-state IgG_1 production. (**A**) Cell retention performance of the microfluidic cell retention device. Error bars, data range (n = 3). (**B**) Glucose and lactate concentrations in the bioreactor. Error bars, data range (n = 3). (**C**) Ammonium (NH_4^+) concentration in the bioreactor. Error bars, data range (n = 3). (**D**) pH and DO concentrations in the bioreactor.

The total cell concentrations in the bioreactor and the harvest bottle were compared throughout perfusion culture to measure cell retention capability. The average total cell concentrations in the bioreactor and harvest bottle were (23.2 ± 0.9) million cells/mL and (2.9 ± 1.1) million cells/mL, respectively (average ± s.d., n = 16). In terms of total number of cells, cell retention efficiency was 98.6% ± 0.7% (average ± s.d., n = 18). The glucose, lactate, and ammonium concentrations were stable over cultivation time. The saturated concentrations for glucose, lactate, and ammonium were (0.18 ± 0.04) g L^{-1}, (2.71 ± 0.10) g L^{-1}, and (1.05 ± 0.05) mM, respectively. (average ± s.d., n = 14). pH and DO were set to 7.0 and 40% (relative to saturation) with the bioreactor controller (BIOSTAT® A PLUS, Sartorius Stedim North America Inc.). DO dropped to 0% after day 6 because high-concentration cell culture consumed oxygen completely. Oxygen supply was limited by aeration and agitation conditions. Despite oxygen limitation, cell culture maintained high viable cell concentration and viability thereafter.

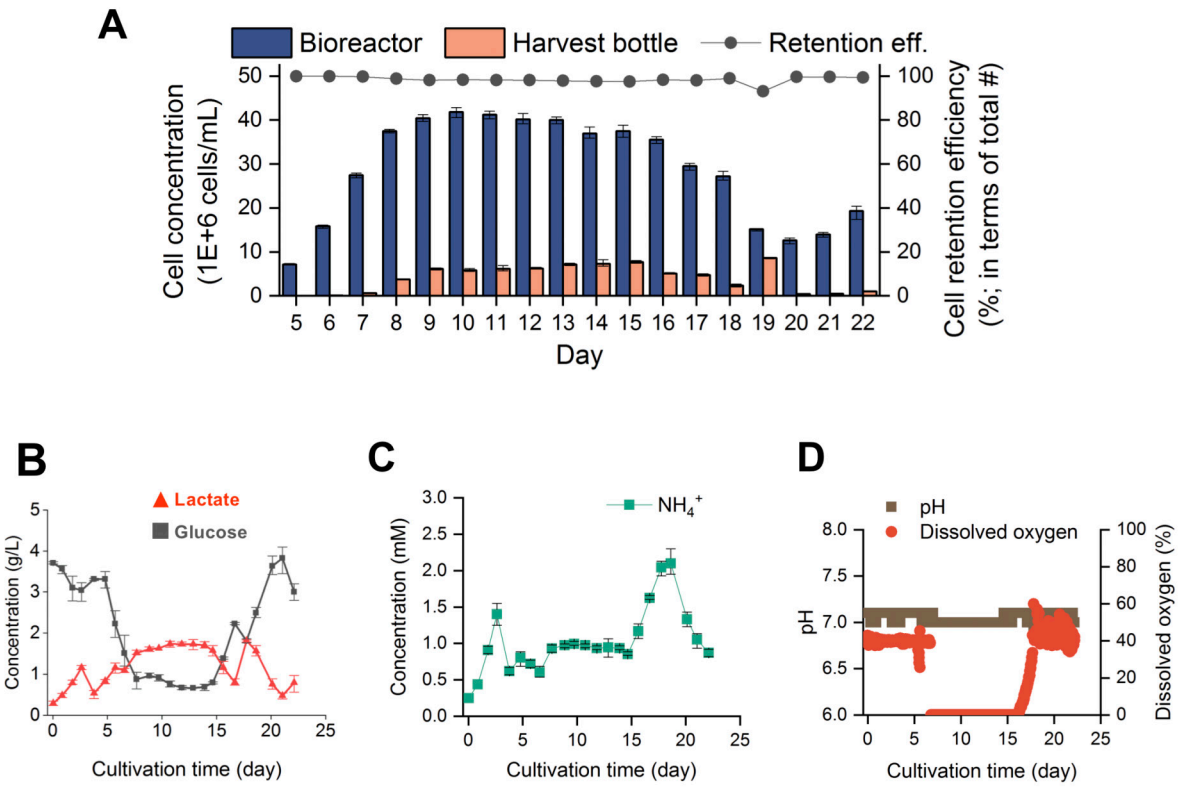

Figure S10. Microfluidic cell retention performance and culture results during transient-state IgG_1 production. (**A**) Cell retention performance of the microfluidic cell retention device. Error bars, data range (n = 3). (**B**) Glucose and lactate concentrations in the bioreactor. Error bars, data range (n = 3). (**C**) Ammonium (NH_4^+) concentration in the bioreactor. Error bars, data range (n = 3). (**D**) pH and DO concentrations in the bioreactor.

The average total cell concentrations in the bioreactor and harvest bottle during day 9 and 13 were (40.7 ± 0.8) million cells/mL and (6.3 ± 0.5) million cells/mL, respectively (average ± s.d., n = 5). In terms of total number of cells, cell retention efficiency was 98.4% ± 1.6% (average ± s.d., n = 18). Glucose and lactate concentrations were maintained at 0.8 ± 0.1 g L^{-1} and 1.7 ± 0.1 g L^{-1} until day 14.6. The ammonium concentration was stable (0.94 ± 0.04) mM (average ± s.d., n = 8) during day 7.7 and 14.7. It then increased to the maximal level (2.1 mM) on day 18.6. After this point, the concentration decreased and returned toward 0.87 mM on day 22.1. pH and DO were set to 7.0 and 40% (relative to saturation) with the bioreactor controller (BIOSTAT® A PLUS, Sartorius Stedim North America Inc.). DO dropped to 0% after day 6.7 because high-concentration cell culture consumed oxygen completely. Oxygen supply was limited by aeration and agitation conditions during day 6.8 to 16.0. The oxygen level returned back to 40% on day 17.9 due to decreased viable cell concentration in the bioreactor.

Section 4. Nanofluidic monitoring results.

Table S2. Summary of the monitoring results during perfusion culture.

Perfusion culture #1 (steady-state; monitoring period: day 11 to 16)						
	Nanofluidic device (*n* = 38)			**Microchip electrophoresis (*n* = 5)**		
	LMWP	**Target**	**HMWP**	**LMWP**	**Target**	**HMWP**
Signal intensity (a.u.)†	0.4 ± 0.0	1.9 ± 0.2	1.4 ± 0.2	689.1 ± 252.7	5079.5 ± 666.1	963.3 ± 90.1
Coefficient variation (%)*	11.4	10.9	13.9	36.7	13.1	9.4
Proportion (%)§	9.6 ± 0.6	51.4 ± 2.0	39.0 ± 1.8	10.0 ± 2.3	75.6 ± 1.8	14.4 ± 1.2
Perfusion culture #2 (transient-state; monitoring period: day 5 to 12)						
	Nanofluidic device (*n* = 50)			**Microchip electrophoresis (*n* = 7)**		
	LMWP	**Target**	**HMWP**	**LMWP**	**Target**	**HMWP**
Signal intensity (a.u.)	0.2 ± 0.0	1.8 ± 0.4	1.1 ± 0.2	357.0 ± 129.2	3412.3 ± 1154.3	571.6 ± 240.3
Coefficient variation (%)	14.7	21.0	17.2	36.2	33.8	42.0
Proportion (%)	6.8 ± 2.7	57.1 ± 5.7	36.1 ± 6.0	8.3 ± 0.9	79.0 ± 1.8	12.7 ± 1.6
Perfusion culture #2 (transient-state; monitoring period: day 17 to 23)						
	Nanofluidic device (*n* = 38)			**Microchip electrophoresis (*n* = 5)**		
	LMWP	**Target**	**HMWP**	**LMWP**	**Target**	**HMWP**
Signal intensity (a.u.)	0.7 ± 0.1	1.5 ± 0.4	0.9 ± 0.2	578.2 ± 181.1	4012.0 ± 1276.3	593.4 ± 240.8
Coefficient variation (%)	15.1	24.9	17.2	31.3	31.8	40.6
Proportion (%)	22.5 ± 2.3	61.1 ± 2.3	16.3 ± 2.3	11.2 ± 1.7	77.5 ± 1.5	11.3 ± 2.5

†, §Signal intensity and proportion were represented by average ± standard deviation (s.d.).

*Coefficient variation is defined as the ratio of standard deviation to average.

Section 5. Online sample preparation test, technology comparison, and monitoring delay.

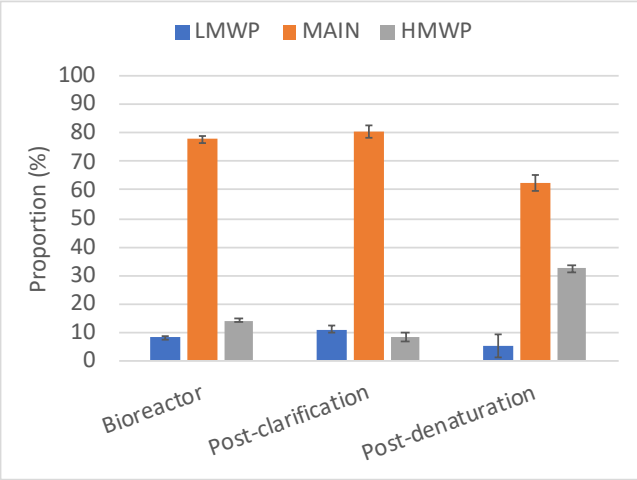

Figure S11. Test of online sample preparation in terms of proportion of each size group. (Bioreactor: cell culture supernatant containing IgG_1, post-clarification: samples obtained after online buffer exchange and cell clarification, post-denaturation: samples obtained after online denaturation; LMWP: Low-molecular-weight proteins (<15kDa), MAIN: Main proteins (15-100kDa), HMWP: High-molecular-weight proteins (>100kDa); Error bars are standard deviations (n = 3, technical replicates))

To compare denaturation effects by online and offline methods, we prepared three different types of samples, such as raw culture supernatant (Bioreactor), the sample after online buffer exchange and cell clarification (Post-clarification), and the sample after online denaturation (Post-denaturation). All samples were analyzed by offline gel electrophoresis microchip (Agilent 2100 Bioanalyzer). The bioreactor and post-clarification samples were denatured using an offline denaturation method, while the post-denaturation sample was not additionally denatured, because it was already denatured through the online denaturation step (**Figure S11**). The result shows that the post-denaturation sample had more HMWP (32.5%) and less MAIN (62.4%) than the bioreactor and post-clarification samples, noting that the online denaturation method was incomplete, compared with the offline method.

To identify the cause of incomplete online denaturation, first, standard IgG_1 was tested (see below; **Figure S12**). Standard IgG_1 was denatured through the online system (65 °C using a ceramic heater). In the online sample preparation system, the final DTT concentration after mixing with labeled proteins was 7.9mM. At this DTT concentration, 45.6% MAIN and 48.8%

HMWP were obtained. On the other hand, when the DTT concentration was increased (31.6mM, 4-fold), 79.7% MAIN and 20.3% HMWP were observed, which was closer to the results from the offline denaturation method (88.3% MAIN and 8,8% HMWP) (offline denaturation method: 11.3mM final DTT concentration). The cell culture supernatant containing IgG_1 showed a similar trend. At 7.9mM DTT concentration, 62.4% MAIN and 32.5% HMWP were obtained. However, at 31.6mM DTT concentration, the proportions of MAIN and HMWP were 69.1% and 23.1%, respectively. These results mean that the higher proportion of HWMP in the perfusion cultures could be due to incomplete denaturation of IgG_1 on the online sample preparation system.

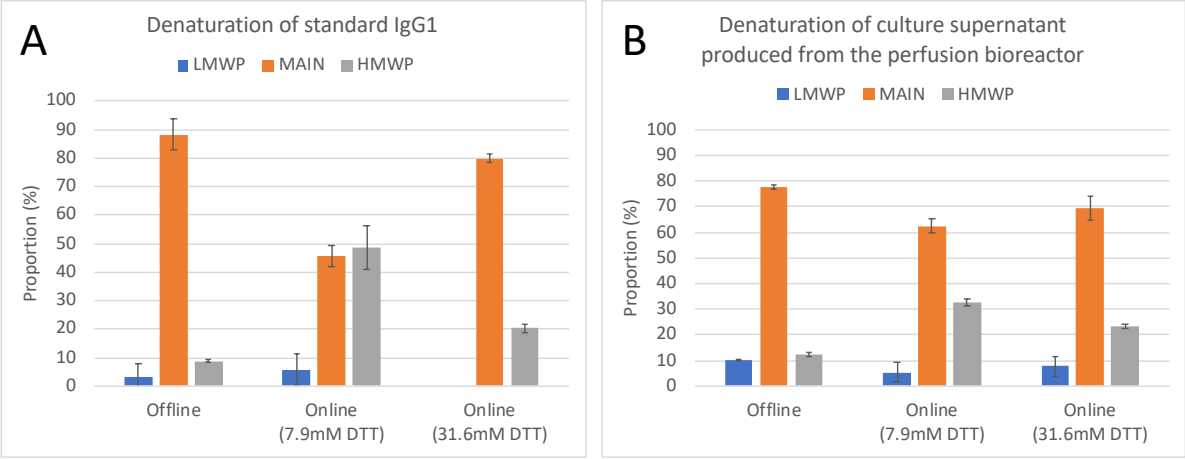

Figure S12. Offline and online denaturation of standard IgG_1 and culture supernatant produced from the perfusion bioreactor. Online denaturation using 7.9mM DTT was used for perfusion culture experiments. (LMWP: Low-molecular-weight proteins (<15kDa), MAIN: Main proteins (15-100kDa), HMWP: High-molecular-weight proteins (>100kDa); Error bars are standard deviations (n = 3, technical replicates))

Table S3. Comparison with other technologies (mAb fragment and aggregation).

Please see the next page.

Technology	Ref.	Mode*	Original sample	Detection target	Denaturation	Online sample preparation	Sample flow continuity	Automation	Monitoring delay	Advantage	Drawback
Nanofluidic filter array	Current work	Online	Cell culture supernatant containing IgG_1	Low molecular weight proteins (<15kDa), main proteins (15-100kDa), high molecular weight proteins (>100kDa)	SDS-heat denaturation under reducing condition	Buffer-exchange, cell clarification, protein labeling, protein denaturation	Continuous from the bioreactor to the nanofluidic analysis device	Fully automated sample preparation and analysis	~5 h (due to sample preparation)	• Directly applied to cell culture samples in the bioreactor • Can be applied to other CQAs (*e.g.*, folding, binding affinity)	• Monitoring delay due to non-optimized sample preparation • Not tested with native IgG
Size-exclusion ultra-high performance liquid chromatography (SE-UHPLC)	• Yang *et al*. (2015)[2]	At-line/ Offline	• Six mAbs (IgG_1 and IgG_4)	Low molecular weight species (mAb Fab/c fragments), main peak (mostly monomer), high molecular species	No denaturation (native mAb forms)	N/A	HPLC vial (by an autosampler), sample loop, and flow-cell (possible to collect mAb fraction using a fraction collector)	Automated analysis on the UHPLC system	<10 min (sampling and analysis)	• Improved resolution and throughput (three times higher) compared with conventional SEC method	• Not applied directly to cell culture samples
Ultra-pressure liquid chromatography size-exclusion separation combined with native electrospray ionization mass spectrometry (UPLC-SEC-MS)	•Haberger *et al*. (2016)[3]	At-line /offline	Bispecific antibody (CrossMAb) samples	Bispecific antibody aggregate and fragment variants (monomers, dimers, light chains and other fragments)	Denatured using electrospray medium or analyzed under native MS conditions (ammonium acetate)	N/A	Sampling, analysis in a flow-cell (UPLC), electrospray ionization, and mass spectrometry	Automated analysis on the UHPLC system, electrospray ionization, and mass spectrometry	<20 min (sampling and analysis)	• Accurate determination of the molecular mass of an analyte • Improved separation resolution	• Not applied directly to cell culture samples
At-line fluorescence spectroscopy with labeled dyes	•Paul *et al.* (2015)[4]	At-line/ offline	Cell culture supernatant (CHO DG44 cell line producing mAb)	mAb aggregates	No denaturation (native mAb forms)	N/A	N/A (analyzed by a microplate reader after manual sample loading)	Automated sample analysis	? (dye incubation time unknown)	• Applied to cell culture samples • High-throughput screening is possible	• Aggregation profile may be sample buffer formulation-specific
At-line fluorescence spectroscopy with labeled dyes	•Paul *et al.* (2017)[5]	At-line /offline	Four different mAbs and one Fab fragment	Aggregates in the size range 1 to 1000 um	No denaturation (native mAb forms)	N/A	N/A (analyzed by a fluorescence microscope after manual sample loading)	Automated sample analysis	? (dye incubation time unknown)	• High-throughput based on automated microscopy imaging	• Not applied directly to cell culture samples

GroEL-BLI Biosensor (Chaperonin-based bio-layer interferometry platform detects partial folds of antibodies)	• Pace *et al.* (2018)[6]	At-line/offline	mAb (IgG_1, IgG_4, bispecific)	Partially structurally altered intermediates (preaggregates)	No denaturation (native mAb forms)	N/A	N/A (analyzed by biolayer interferometry equipment after manual sampling loading)	Automated sample analysis	<30 min (analysis)	• High-throughput based on automated analysis • mAb pre-aggregation forms can be detected	• Not applied directly to cell culture samples • Complex calibration is required

* The definition of mode of operation (online, inline, at-line, and offline) was introduced in a document published by BioPhorum Operations Group[7]. (Online: "the sample is diverted from the process and may be returned to the process stream", Inline: "the sample is not removed from the process stream", at-line: "the sample is removed, isolated from and analyzed near to the process stream", offline: "the sample is tested in a conventional quality control (QC) lab outside of the production area")

Table S4. Processing time delay of online sample preparation and possible solutions.

Sample preparation step	Processing time	Potential causes of the delayed processing time	Example Solutions	Target processing time
Buffer exchange	**~30 min** (diafiltration of protein solution through a hollow fiber membrane)	Long hollow fiber due to a low exchange rate through the membrane	• Use higher flow rates for the exchange buffer to increase ion exchange rate[8]	<10 min
Cell clarification	**~30 min** (microfiltration by a membrane filter)	Dead volume of the membrane filter with low flow rate	• Use the membrane filter with small dead volume with high flow rate • Use membrane-less microfluidic clarification devices[1]	<1 min
Protein labeling	**~60 min** (mixing and incubation of proteins and fluorescence dye at room temperature)	Long capillary tube with a large inner diameter to mix samples by diffusion only (fluctuated sample flow by the peristaltic pump)	• Use peristaltic pumps with low flow fluctuation • Use a micromixer to improve mixing efficiency • Use higher flow rates for the exchange buffer to increase ion exchange rate[8] • Use label-free protein detection methods (UV, Raman, *etc*.)	<20 min
	~30 min (free dye removal through a hollow fiber membrane)	Long hollow fiber due to low exchange rate through the membrane		
Denaturation	**~60 min** (mixing of labeled proteins and denaturation solution)	Long capillary tube with a large inner diameter to mix samples by diffusion only (fluctuated sample flow by the peristaltic pump)	• Use peristaltic pumps with low flow fluctuation • Use a micromixer to improve mixing efficiency • Incubate samples at higher temperature	<20 min
	~30 min (incubation on the heater)	Capillary tube with a large inner diameter for long-term exposure to thermal energy for denaturation		
Other	**~60 min** (sample flow between sample preparation steps through capillary tubes)	Long capillary tube to connect with each sample preparation step	• Replace capillary-based system with microfluidic-based system	<10 min

Section 6. Effect of electric field strength on separation performance of the nanofluidic device.

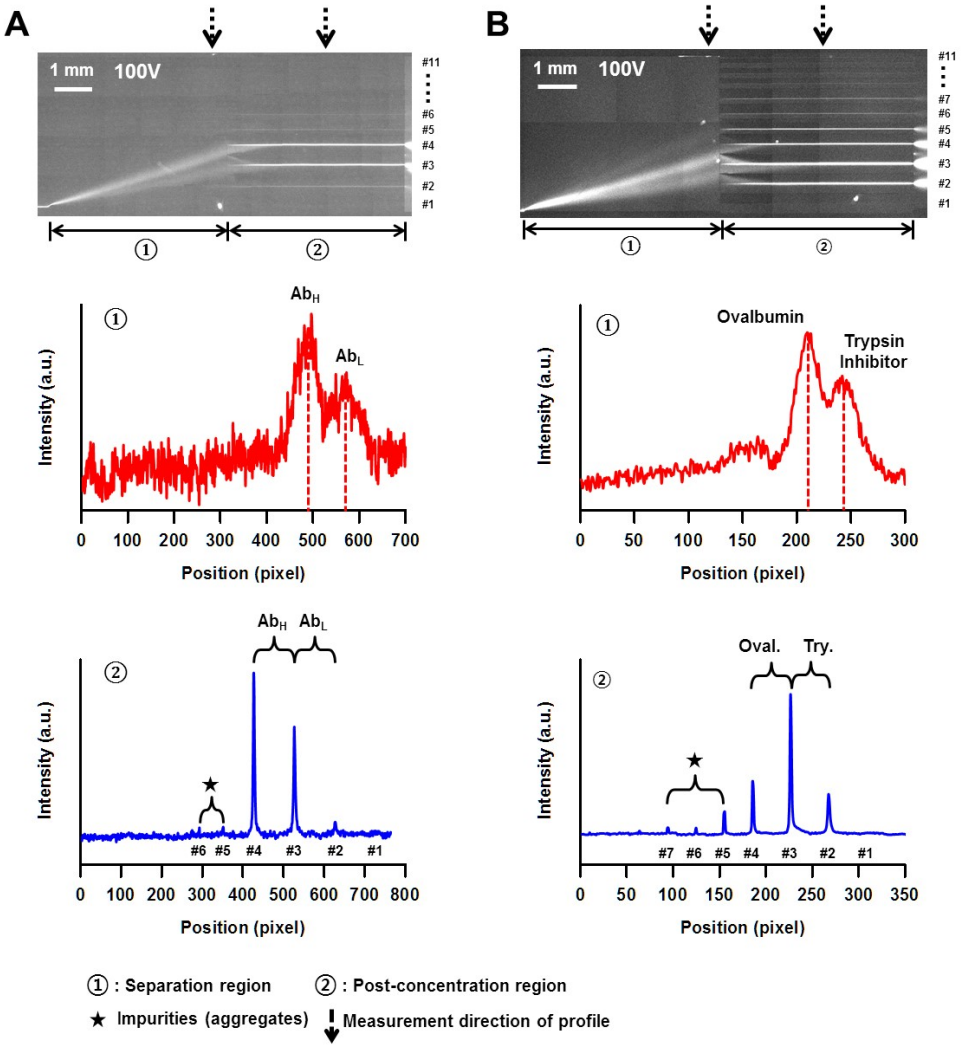

Figure S13. Offline separation of IgG_1 and protein mixture in the nanofluidic device at 100 V. (**A**) IgG_1 (light chains: 25 kDa; heavy chains: 50 kDa). (**B**) Ovalbumin (44.3 kDa) and trypsin inhibitor (20.1 kDa). Fluorescence images for proteins' behavior in the nanofluidic device and fluorescence signal profiles of separated proteins in the separation region (①) and in the post-concentration region (②). 100 V was applied to the filter array. All the proteins were fluorescently labeled and denatured using SDS and DTT.

Separation performance of biomolecule mixtures is affected by electric field strength (voltage)

An additional feature of the nanofluidic device is that the separation performance of biomolecule mixtures is affected by electric field strength (voltage).[9,10] To check the effect of electric field strength on device performance, separation performance of IgG_1 and protein size markers was compared under different voltage strengths. The peak distance (size selectivity) between Ab_L and Ab_H or ovalbumin and trypsin inhibitor in the separation region increased as the voltage was decreased. On the other hand, in the post-concentration region, the channel numbers (position) collecting target proteins were independent of the range of voltage strength applied in this work, such as 100 V and 200 V (**Figure 2B**; **Figure S7A** and **Figure S13**). In addition to size selectivity, the applied voltage also influences separation speed. As 200 V provided comparable separation performance to 100 V in the post-concentration region and higher separation speed than 100 V, 200 V was used for online monitoring experiments. Voltages over 200 V induced electrical breakdown of the nanofluidic device.

Section 7. Figure data.

Table S5. Figure data for Figure 4 and 5.

Figure 4A

Time [day]	Viable concentration [×10^6 cells/mL]			Viability [%]		
	Sample 1	Sample 2	Sample 3	Sample 1	Sample 2	Sample 3
0.0	0.5	0.5	0.5	95	93	94
1.1	0.6	0.5	0.7	87	84	90
2.0	1.5	1.5	1.4	95	94	93
2.8	3.6	3.3	3.3	99	96	95
4.1	8.3	8.4	8.2	99	97	97
4.9	15.6	15.5	15.1	99	97	97
5.9	23.4	24.0	26.5	98	98	99
6.8	27,9	27.3	25.6	99	97	96
8.1	26.4	26.4	25.3	98	97	98
9.2	26.9	26.8	25.7	98	97	97
10.1	26.2	25.4	25.8	98	97	97
10.9	26.8	26.3	25.4	98	97	97
12.0	28.5	27.5	27.7	97	96	96
13.3	25.3	25.1	24.9	95	95	95
14.2	26.6	25.2	25.7	94	93	93
15.0	25.2	25.3	25.1	92	92	92
16.0	27.6	25.3	24.6	95	95	94
17.2	29.2	26.7	26.1	95	95	94
18.1	27.7	25.0	25.5	94	94	94
18.9	22.5	24.1	24.1	94	93	94
20.1	23.7	24.2	24.3	93	93	93
21.2	23.1	23.9	23.6	95	96	96

Figure 4D

Time [day]	Offline microchip [Total amount of proteins, unit: a.u.]		
	Sample 1	Sample 2	Sample 3
12.0	6477.2	4459.1	4783.3
13.3	8496.1	4600.6	6656.2
14.2	5816.7	7887.2	6556.6
15.0	7952.3	9230.4	6517.1
16.1	7366.6	7656.3	6522.2

Figure 4F

Time [day]	Offline microchip [Amount of proteins, unit: a.u.]								
	LMWP (<15 kDa)			Target (15-100 kDa)			HMWP (>100 kDa)		
	Sample 1	Sample 2	Sample 3	Sample 1	Sample 2	Sample 3	Sample 1	Sample 2	Sample 3
12.0	568.7	353.2	239.2	4937.5	3527.6	3497.6	970.9	578.4	1046.6
13.3	760.4	525.4	605.7	6435.8	3469.3	5201.2	1299.9	605.9	849.3
14.2	528.2	821.1	620.3	4428.8	5966.7	5118.7	859.7	1099.5	817.6
15.0	1688.3	842.7	735.1	5211.1	7053.0	4890.4	1052.9	1334.7	891.5
16.1	667.4	807.7	573.3	5597.1	5694.0	5163.0	1102.0	1154.6	785.9

Figure 5A

Time [day]	Viable concentration [×10^6 cells/mL]			Viability [%]		
	Sample 1	Sample 2	Sample 3	Sample 1	Sample 2	Sample 3
0.0	0.4	0.4	0.3	99	97	97
0.8	0.8	0.6	0.6	96	97	97
1.8	1.7	1.4	1.4	99	98	99
2.6	3.3	3.2	3.3	98	98	98
3.8	3.0	2.9	2.8	96	96	97
4.8	7.3	7.0	6.9	99	99	99
5.7	15.8	15.2	16.0	99	99	99
6.6	27.4	27.6	26.7	99	99	99
7.7	37.5	37.2	36.7	99	99	99
8.9	40.8	39.9	39.3	99	99	99
9.7	42.3	40.0	41.6	99	98	98
10.7	41.5	40.9	39.8	99	99	99
11.8	41.0	38.7	39.3	99	99	99
12.9	37.9	39.4	39.0	97	97	97
13.9	36.0	35.4	37.8	98	99	98
14.7	36.4	35.2	33.7	94	94	93
15.6	33.6	32.7	34.1	94	94	94
16.7	26.6	28.0	28.2	93	94	94
17.7	22.9	23.3	24.7	87	87	87
18.6	12.4	12.2	12.4	81	82	81
20.1	7.1	6.3	7.1	54	53	55
21.0	8.1	7.6	8.1	56	57	57
22.1	12.9	15.6	15.7	74	77	77
22.7	18.6	19.2	19.3	83	84	84

Figure 5D

Time [day]	Offline microchip [Total amount of proteins, unit: a.u.]		
	Sample 1	Sample 2	Sample 3
5.7	2483.9	1995.6	2606.2
6.6	2472.6	2106.8	2330.9
7.7	5397.3	3250.2	3809.4
8.9	6481.3	5600.3	4389.3
9.7	6561.8	5847.1	5385.6
10.7	6177.9	5854.0	5044.0
11.8	4500.2	4945.9	3919.9
17.7	7715.2	8042.8	7256.8
18.6	5992.7	5634.3	6244.3
20.1	4527.8	4643.1	3617.3
21.0	5428.4	4341.8	3765.2
22.1	3016.4	3461.6	4066.1

Figure 5F

Time [day]	Offline microchip [Amount of proteins, unit: a.u.]								
	LMWP (<15 kDa)			Target (15-100 kDa)			HMWP (>100 kDa)		
	Sample 1	Sample 2	Sample 3	Sample 1	Sample 2	Sample 3	Sample 1	Sample 2	Sample 3
5.7	210.3	203.3	245.1	2009.6	1651.2	2049.3	264.0	141.1	311.8
6.6	83.0	184.2	242.0	2093.2	1723.3	1780.4	296.4	199.3	308.5
7.7	352.9	239.6	279.1	4328.1	2610.8	3093.6	716.3	399.8	436.7
8.9	494.4	440.1	388.7	5125.8	4466.4	3367.5	861.1	693.8	633.1
9.7	521.7	507.0	409.4	5179.1	4580.6	4221.9	861.0	759.5	754.3
10.7	528.3	490.0	440.5	4737.5	4542.5	3863.0	912.1	821.5	740.5
11.8	449.4	419.8	368.7	3421.5	3843.7	2970.0	629.3	682.4	581.2
17.7	756.8	812.8	732.8	6080.6	6185.8	5617.7	877.8	1044.2	906.3
18.6	639.4	618.1	1046.0	4796.8	4509.3	4505.7	556.5	506.9	692.6
20.1	583.6	531.4	503.9	3389.8	3709.9	2710.9	554.4	401.8	402.5
21.0	451.9	407.8	360.9	4170.6	3295.8	2808.2	805.9	638.2	596.1
22.1	333.0	385.1	509.9	2446.6	2783.4	3168.4	236.8	293.1	387.8

References

(1) Kwon, T.; Prentice, H.; Oliveira, J. De; Madziva, N.; Warkiani, M. E.; Hamel, J.-F. P.; Han, J. *Sci. Rep.* **2017**, *7*, 6703.

(2) Yang, R.; Tang, Y.; Zhang, B.; Lu, X.; Liu, A.; Zhang, Y. T. *J. Pharm. Biomed. Anal.* **2015**, *109*, 52–61.

(3) Haberger, M.; Leiss, M.; Heidenreich, A.-K.; Pester, O.; Hafenmair, G.; Hook, M.; Bonnington, L.; Wegele, H.; Haindl, M.; Reusch, D.; Bulau, P. *MAbs* **2016**, *8* (2), 331–339.

(4) Paul, A. J.; Schwab, K.; Prokoph, N.; Haas, E.; Handrick, R.; Hesse, F. *Anal. Bioanal. Chem.* **2015**, *407* (16), 4849–4856.

(5) Paul, A. J.; Bickel, F.; Röhm, M.; Hospach, L.; Halder, B.; Rettich, N.; Handrick, R.; Herold, E. M.; Kiefer, H.; Hesse, F. *Anal. Bioanal. Chem.* **2017**, *409* (17), 4149–4156.

(6) Pace, S. E.; Joshi, S. B.; Esfandiary, R.; Stadelman, R.; Bishop, S. M.; Middaugh, C. R.; Fisher, M. T.; Volkin, D. B. *J. Pharm. Sci.* **2018**, *107* (2), 559–570.

(7) Swann, P.; Brophy, L.; Strachan, D.; Lilly, E.; Jeffers, P. *Biomanufacturing Technology Roadmap-In-line monitoring and real-time release*; Tech. rep., BioPhorum Operations Group Ltd, 2017.

(8) Sun, L.; Duan, J.; Tao, D.; Liang, Z.; Zhang, W.; Zhang, L.; Zhang, Y. *Rapid Commun. Mass Spectrom.* **2008**, *22* (15), 2391–2397.

(9) Fu, J.; Mao, P.; Han, J. *Appl. Phys. Lett.* **2005**, *87* (26), 263902.

(10) Fu, J.; Schoch, R. B.; Stevens, A. L.; Tannenbaum, S. R.; Han, J. *Nat. Nanotechnol.* **2007**, *2* (2), 121–128.